



Accepted Article

Title: Synthesis of new Tyrosol-based Phosphodiester Derivatives: effect on amyloid β aggregation and metal chelation ability.

Authors: Valeria Romanucci, Maddalena Giordano, Gaetano De Tommaso, Mauro Iuliano, Roberta Bernini, Mariangela Clemente, Sara Garcia-Viñuales, Danilo Milardi, Armando Zarrelli, and Giovanni Di Fabio

This manuscript has been accepted after peer review and appears as an Accepted Article online prior to editing, proofing, and formal publication of the final Version of Record (VoR). This work is currently citable by using the Digital Object Identifier (DOI) given below. The VoR will be published online in Early View as soon as possible and may be different to this Accepted Article as a result of editing. Readers should obtain the VoR from the journal website shown below when it is published to ensure accuracy of information. The authors are responsible for the content of this Accepted Article.

To be cited as: *ChemMedChem* 10.1002/cmdc.202000807

Link to VoR: <https://doi.org/10.1002/cmdc.202000807>

Synthesis of new Tyrosol-based Phosphodiester Derivatives: effect on amyloid β aggregation and metal chelation ability.

Valeria Romanucci,^{[a]‡} Maddalena Giordano,^{[a]‡} Gaetano De Tommaso,^[a] Mauro Iuliano,^[a] Roberta Bernini,^[b] Mariangela Clemente,^[b] Sara Garcia-Viñuales,^[c] Danilo Milardi,^[c] Armando Zarrelli,^[a] and Giovanni Di Fabio*^[a]

- [a] Dr. V. Romanucci, Dr. M. Giordano, Dr. G. De Tommaso, Prof. M. Iuliano, Prof. A. Zarrelli, Dr. G. Di Fabio
Department of Chemical Sciences
University of Napoli Federico II
Via Cintia 4, I-80126 Napoli, Italy
E-mail: valeria.romanucci@unina.it, maddalena.giordano@unina.it, gaetano.detommaso@unina.it, mauro.iuliano@unina.it, zarrelli@unina.it, difabio@unina.it
- [b] Prof. R. Bernini, Dr. M. Clemente
Department of Agriculture and Forest Science (DAFNE)
University of Tuscia
Via S. Camillo De Lellis, 01100 Viterbo, Italy
E-mail: roberta.bernini@unitus.it, marian.clem@unitus.it
- [c] Dr. D. Milardi, Dr. S. Garcia-Viñuales
Istituto di Cristallografia
Consiglio Nazionale delle Ricerche
Via Paolo Gaifami 18, 95126 Catania, Italy
E-mail: sara.garciavinuales@ibb.cnr.it, danilo.milardi@cnr.it

* These authors contributed equally.

Supporting information for this article is given via a link at the end of the document. ((Please delete this text if not appropriate))

Abstract: Alzheimer's disease (AD) is a multifactorial pathology that requires multifaceted agents able to address its peculiar nature. Increasing evidence has shown that aggregation of amyloid- β (A β) and oxidative stress are strictly interconnected, and their modulation may have a positive and synergic effect in contrasting AD-related impairments. Herein, a new and efficient fragment-based approach towards Tyrosol Phosphodiester Derivatives (TPDs) has been developed starting from suitable tyrosol building blocks and exploiting the well-established phosphoramidite chemistry. The antioxidant activity of new TPDs has been tested as well as their ability to inhibit A β protein aggregation. In addition, it has been evaluated their metal chelating ability as a possible strategy to develop new natural-based entities for the prevention or therapy of AD. Interestingly, the TPDs containing the catecholic moiety have demonstrated a highly promising activity in inhibiting aggregation of A β ₄₀ and a strong ability to chelate bio-metals such as Cu (II) and Zn (II).

Introduction

Natural products from different source organisms continue to inspire most drug leads for many diseases. On average, about half of the new drugs (small molecules) approved by the FDA, stem directly from natural sources or by a synthesis inspired by natural molecular motifs.^[1]

In this frame, polyphenols are a class of micronutrients which have shown a growing interest due to their effects in the prevention and treatment of different illnesses, particularly cancer, diabetes, inflammation, liver disease, cardiovascular disease, cataract, nephrotoxicity and neurodegenerative diseases. The health-promoting effects appear to be linked to their strong antioxidant activity which reduces the occurrence of different age-

related disorders.^{[2],[3]} Oxidative stress may induce cellular damage, impairment of the DNA repair system, and mitochondrial dysfunction, all of which have been known as key factors in the acceleration of the aging process and the development of neurodegenerative disorders, including Alzheimer's disease (AD), Parkinson's disease (PD), multiple sclerosis (MS), Huntington's disease (HD), and amyotrophic lateral sclerosis (ALS).^{[4],[5]} Alzheimer's disease is the most common neurodegenerative disorder worldwide, described by the progressive impairment of cognitive abilities leading to dementia and death.^[6] Several factors, such as cholinergic dysfunction, deposits of amyloid- β (A β) protein, oxidative stress as well as reduced blood supply in the brain, are supposed to be relevant for its development and for the degeneration in the disease. Intracellular deposits of hyperphosphorylated tau (τ) protein^[7] and extracellular aggregates of the amyloid- β peptides (A β) are the pathological hallmarks of AD. What causes this abnormal accumulation of proteinaceous deposits is still unclear, but among the hypotheses, one of the most widely accepted is known as "the amyloid hypothesis". This hypothesis invokes the participation of amyloid precursor protein (APP) in neuronal cell death and postulates that the deposition of partially aggregated soluble A β triggers a neurotoxic cascade, thereby causing neurodegeneration and AD.^{[8],[5],[9]} Many studies report accelerated rates of A β aggregation in the presence of certain divalent metal cations such as Cu (II) and Zn (II). Metal ions might participate in A β -induced oxidative stress through their redox cycling while bound to A β peptide. Redox-active metals (e.g., copper, iron) associated with A β species have been involved in Fenton-like chemistry, causing oxidative stress and neuronal damage. These cations interfere not only in metal-induced A β aggregation and neurotoxicity, but also on metal homeostasis of AD brains.^{[10],[11],[12],[13]}

FULL PAPER

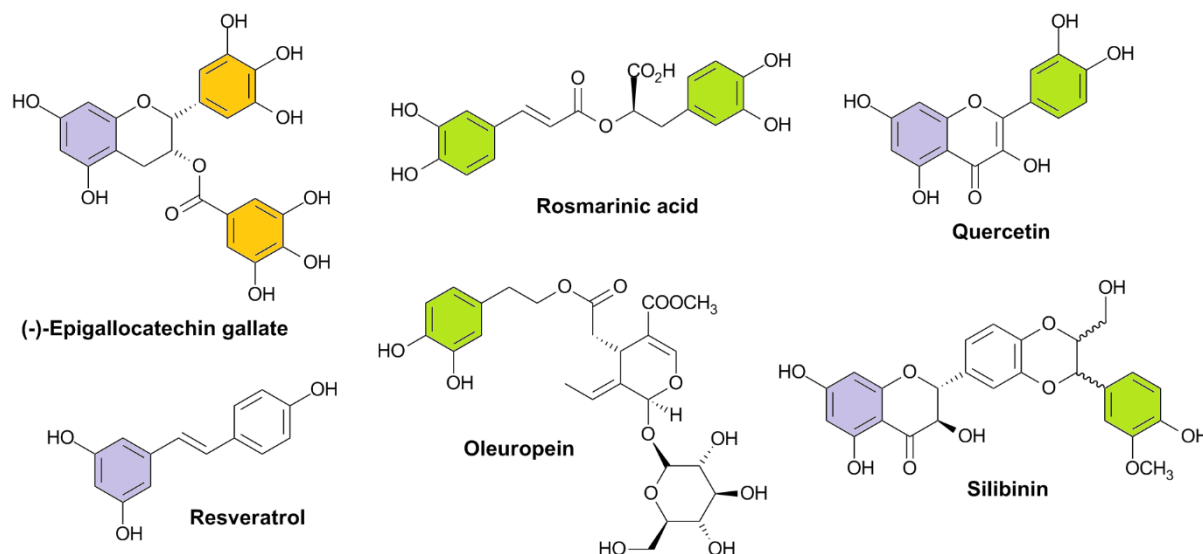


Figure 1. Natural polyphenols with β -amyloid anti-aggregation properties.

Compounds that show both radical scavenging activity and capacity for bio-metal modulation in the brain may be useful for both prevention and therapy of AD. Metabolites such as epigallocatechin gallate, resveratrol, rosmarinic acid, oleuropein, silibinin and quercetin (Fig. 1), containing catecholic or pyrogallol rings, showed a disrupting effect on A β aggregation. All compounds share some structural motifs crucial for AD activity.^{[14],[15],[16],[17]}

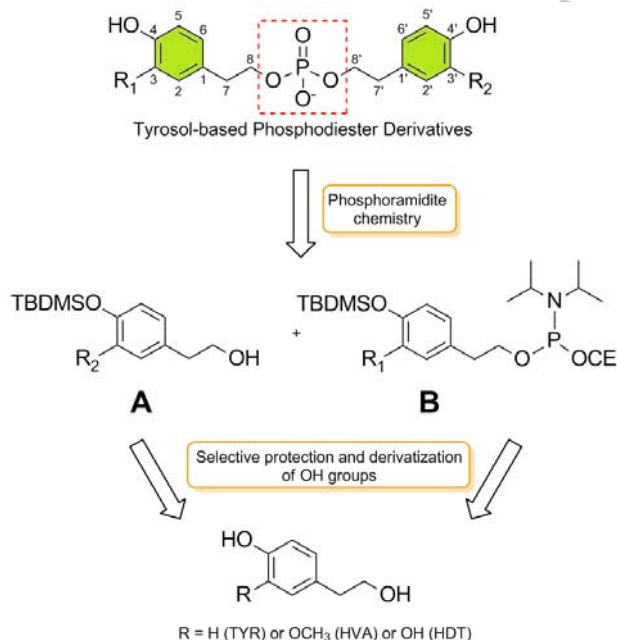
The pharmacological activities of all new compounds were evaluated. TYR and HDT are known for their broad spectrum of pharmacological properties^{[23],[24],[25],[26]} as anti-inflammatory, anticancer^{[27],[28],[29]}, neuroprotective activity^{[30],[31],[32],[33]} and anti-atherosclerotic.^[34]

Herein we report the synthesis and characterization of a mini-library of new tyrosol-based phosphodiester derivatives (TPDs), containing two phenylethanoid fragments linked through a phosphodiester bond (Scheme 1). We have focused our attention to evaluation the behavior of new tyrosol-based derivatives, relatively to different aspects involved in AD pathology: oxidative stress, A β aggregation and role of biometals on A β aggregation. For this purpose, the radical scavenger activity, A β ₄₀ aggregation inhibitory activity and the chelating ability of bio-metals as Cu (II) and Zn (II) were carried out.

Results

Synthesis of tyrosol-based phosphodiester derivatives (TPDs)

For the preparation of a mini library of TPDs, the general design presented herein is based on the coupling of suitable tyrosol building blocks, one of which contains the phosphoramidite function (Scheme 1). The selected tyrosol scaffolds identified as tyrosol (TYR), homovanillyl alcohol (HVA) and hydroxytyrosol (HDT) are combined in order to obtain a variety of linked-phosphodiester dimers. The synthetic route to the target TPD was thus realised by starting from building blocks **A** and **B** (Scheme 1), obtained in two or three straightforward steps. The TBDMS group was chosen to protect the phenolic functionalities due to the easy installation procedure and above all the mild regio-selective removal conditions with I₂ in MeOH to obtain the building blocks **7** – **9** (Scheme 2). Furthermore, the TBDMS deprotection from full protected dimers (**13** – **18**) can be achieved by mild treatment (Et₃N·3HF) in THF as solvents, which is fully compatible with very sensitive catecholic functions as well as the phosphotriester or diester linkage. TYR (**1**), HVA (**2**) and HDT (**3**),^[35] reacted with an excess of *tert*-butyldimethylsilyl chloride



Scheme 1. Design of Tyrosol-based Phosphodiester Derivatives.

In the last few years, many polyphenols conjugated or derivatives containing catechol units, have been found to have interesting anti-amyloid activity.^{[18],[19],[20],[21],[22]} Here, tyrosol (TYR), homovanillyl alcohol (HVA) and hydroxytyrosol (HDT), have been used as scaffold for the design and synthesis of their conjugates.

FULL PAPER

(TBDMSCI) in DMF in the presence of Et₃N, giving fully protected compounds **4** – **6**. The regioselective deprotection of the TBDMS group was obtained by treating **4** – **6** with I₂/MeOH at room temperature leading to aliphatic alcohols **7** – **9**. The latter ones intermediates were then reacted with 2-cyanoethyl-N,N-diisopropylamino-chlorophosphoramidite in the presence of DIEA, giving target phosphoramidites **10** – **12** in excellent yields (72%, 68% and 90% respectively). All the intermediates have been purified by silica gel chromatography and fully characterized by ¹H, ¹³C, ³¹P (where present) NMR and ESI-MS analysis.

Tyrosol derivatives **7** – **9** were coupled with phosphoramidites **10** – **12** using 4,5-dicyanoimidazole (DCI) as activator reagent. After treatment with 5.5 M *tert*-butyl hydroperoxide (TBHP) solution in decane, the crude material was purified by flash chromatography leading to dimers **13** – **18** in good yields. Different routes were used to remove TBDMS groups depending on the tyrosol units. In particular dimers not containing the catecholic moiety (**13** – **15**) were treated with NaOH in MeOH/H₂O (1:1, v:v) at r.t. (deprotection method A) affording dimers fully deprotected **19** – **21** (75%, 78% and 77% respectively). For the dimers **16** – **18** the TBDMS was removed with the complex (Et₃N·3HF) in THF (deprotection method B) followed by the deprotection of cyanoethyl group (CE), by treatment with NH₄OH/MeOH at r.t., to obtain dimers **25** – **27** (Table 1).

All final compounds (**19** – **21** and **25** – **27**) were obtained by silica gel chromatography (DCM/MeOH 60:40 to 50:50 v/v) in 20 – 46 % average yields. The final TPDs (**19** – **21** and **25** – **27**) then were converted into the corresponding sodium salts by cation exchange on a DOWEX (Na⁺ form) resin. Final compounds were

analysed by HPLC on an analytical RP18 column, showing in all cases one main peak, with a purity of over 97%.

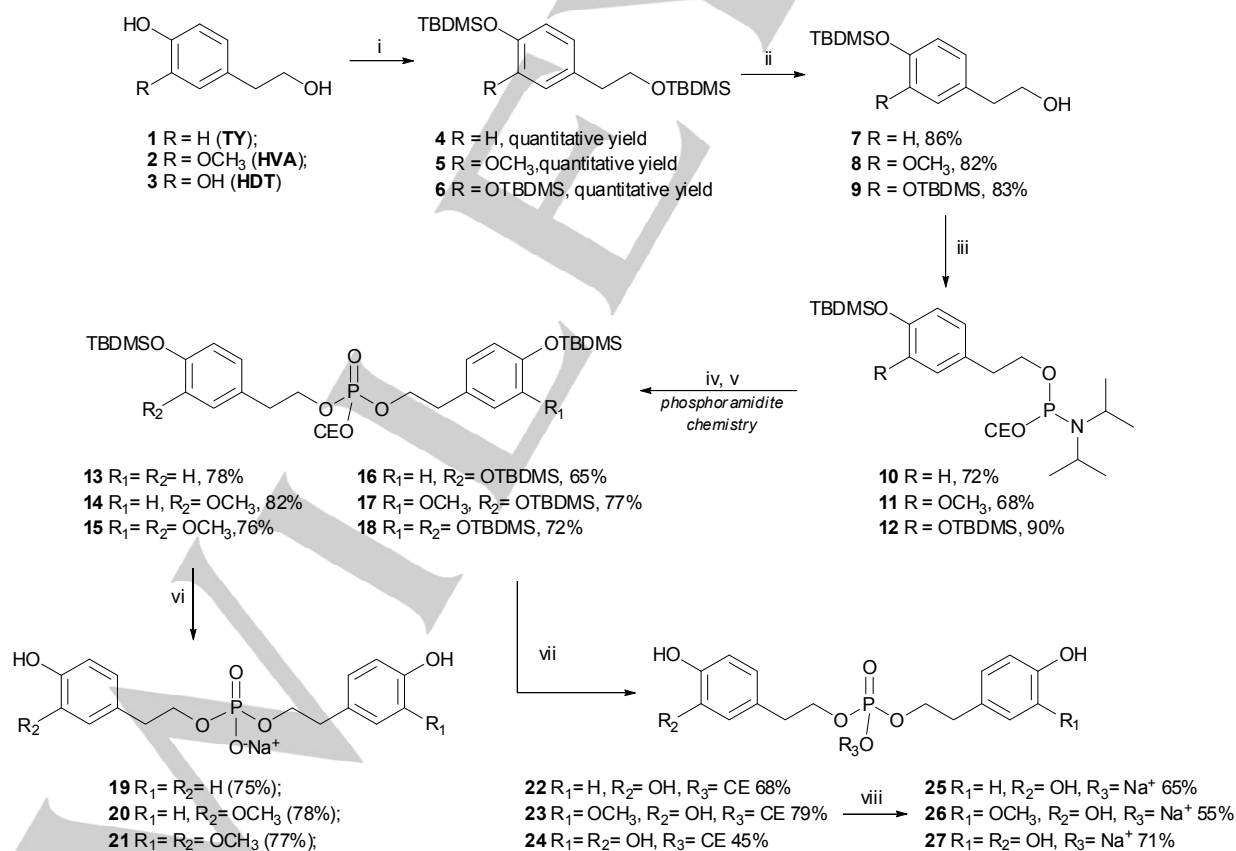
Table 1. Yields and radical scavenger activity of TPDs (**19-21** and **25-27**).

TPD	Total yield (%)	ABTS ^{•+} (TE mM) ^d
TYR- <i>p</i> -TYR (19)	42 ^a	0.97 ± 0.23
TYR- <i>p</i> -HVA (20)	46 ^a	1.21 ± 0.07
HVA- <i>p</i> -HVA (21)	40 ^b	1.43 ± 0.03
HDT- <i>p</i> -TYR (25)	38 ^c	0.66 ± 0.05
HDT- <i>p</i> -HVA (26)	30 ^c	0.65 ± 0.03
HDT- <i>p</i> -HDT (27)	20 ^c	0.69 ± 0.03
TYR (1)		0.45 ± 0.02
HVA (2)		0.81 ± 0.04
HDT (3)		0.68 ± 0.02

^acalculated starting from **10**; ^bcalculated starting from **11**; ^ccalculated starting from **12**; ^dTE: Trolox Equivalent

Radical scavenging properties of TPDs **19** – **21** and **25** – **27** (ABTS^{•+} test)

TPDs **19** – **21** and **25** – **27** were herein screened for their radical scavenging capacity using the *in vitro* ABTS^{•+}[33] and compared to that of the corresponding monomers **1** – **3**.



Scheme 2. Reagents and conditions: (i) TBDMSCI, Et₃N, DMF, r.t., 3 h; (ii) 1% I₂/MeOH, r.t., 3 h; (iii) DIEA, MS 4Å, DCM, r.t., 1 h; (iv) coupling between **7-9** and **10-12**, MS 4Å, DCI, r.t., 3 h; (v) TBHP 5.5M in decane, r.t., 1 h; (vi) NaOH in THF, r.t., 4 h (method A); (vii) Et₃N·3HF, THF, r.t., 3.5 h then (viii) NH₃/MeOH, MeOH, r.t., 30 min (method B).

FULL PAPER

This method is the most used for evaluating the *in vitro* antioxidant activity of phenolic compounds giving reliable results^{[36],[37],[38]}. The experimental data of the ABTS^{•+} assay, expressed as Trolox Equivalent Antioxidant Capacity (TEAC in mM equivalent), of all tested compounds are summarized in Table 1. Among monomers **1** – **3**, TYR (**1**) resulted less effective than both HVA (**2**) and HDT (**3**), showing TEAC values of 0.45 ± 0.02 , 0.81 ± 0.04 and 0.68 ± 0.02 , respectively, according to that previously observed by us.^[38] When it was linked with itself, **2** and **3**, the activity of TYR (**1**) resulted increased; in particular, TYR-*p*-HVA (**20**) showed a TEAC value of 1.21 ± 0.07 . A similar behaviour was observed for HVA in combination with itself and TYR (**1**) observing TEAC

values of 1.43 ± 0.03 and 1.21 ± 0.07 for **21** and **20**, respectively. Unexpectedly, HDT (**3**) linked to **1**, **2** and itself to produce HDT-*p*-TYR (**25**), HDT-*p*-HVA (**26**) and HDT-*p*-HDT (**27**) resulted effective as the respective monomers.

A β Amyloid anti-aggregation behavior of TPDs

To evaluate the ability of TPDs (ligands) to modulate A β ₄₀ aggregation, ThT (Thioflavin T) experiments have been carried out in the absence and presence of increasing concentrations of ligands (peptide/ligand molar ratios 1:0.25, 1:0.5 and 1:1).

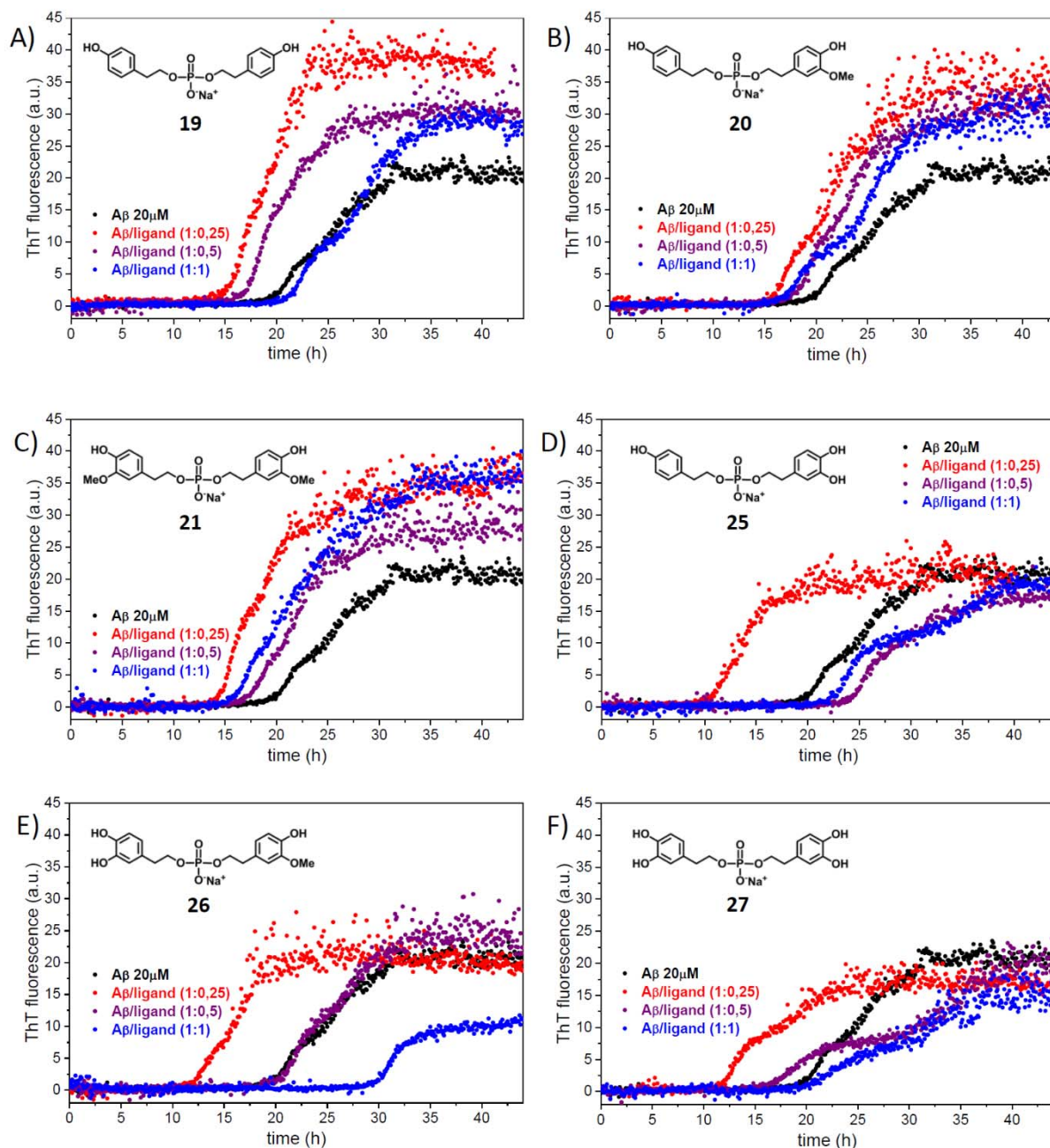


Figure 2. - A β growth kinetics in the presence of different TPDs. A) Amyloid fibrillation kinetics of A β in absence (black curve) and in presence of TYR-*p*-TYR in peptide/ligand molar ratios 1:0.25 (red curve), 1:0.5 (purple curve) and 1:1 (blue curve). Dots represent experimental data; each condition has been tested in triplicate and the characteristic parameters of the kinetics are indicated in supplementary figure S1). Experiments were carried out using A β 20 μ M at 37°C in phosphate buffer 10 mM NaCl 100mM pH 7.4. B) As A) except for TYR-*p*-HVA (**20**). C) As A) except for HVA-*p*-HVA (**21**); D) As A) except for TYR-*p*-HDT (**25**). E) As A) except for HDT-*p*-HVA (**26**); F) As A) except for HDT-*p*-HDT (**27**).

FULL PAPER

Derivatives **19** – **21** which contain two TYR or HVA moieties or a combination of both of them, catalyzed the aggregation phenomenon as the parental monomers. In fact, these compounds reduced the lag phase and increased the total amount of the formed fibers at all tested peptide/ligand ratios (Fig. S1). The effect was more accentuated at 1:0.25 peptide/ligand molar ratio (TYR-*p*-TYR **19**, HVA-*p*-HVA **21** and TYR-*p*-HVA **20**, reduced the lag phase by about 7.5 h, 10.6 h, and 7.2 h, and increased the amount of fibrils by about 82%, 64% and 62%, respectively) and the compounds presented a progressive loss of activity by increasing it (Fig. 2). Interestingly, TPDs that contain the monomer HDT (**25** – **27**), presented a bimodal behavior, producing an acceleration or an inhibition of the aggregation depending on the concentration of the dimer ligand. All of them gave rise to a reduction in the lag phase at the smaller tested peptide/ligand molar ratio 1:0.25 (reduction of about 10.2 h, 8.8 h, and 10.9 h for HDT-*p*-HDT **27**, TYR-*p*-HDT **25**, and HVA-*p*-HDT **26**, respectively) while a slowdown of the kinetics was observed at 1:1 molar ratio (increase in $t_{1/2}$ of about 3.8 h, 4 h, and 9.8 h, respectively), presenting an intermediate effect between both situations at 1:0.5 peptide/ligand molar ratio (Fig. S1). However, the efficacy of inhibiting the aggregation is only present at the higher tested peptide ligand molar ratios (1:1 and in some cases 1:0.5) and the ability to favor the aggregation of HVA and

TYR is able to counterbalance the catechol properties at the smaller tested ratio (1:0.25).

Acid–base behaviour and metal chelating capacity of TPDs

Based on their interesting inhibition of A β growth kinetics (Fig. 2), dimers **25** – **27** were selected for further characterization. In particular, considering that the catecholic motif in TPDs **25** – **27** makes them potential chelating agents, their ability to complex Cu (II) and Zn (II) ions have been evaluated. To investigate the chelating capacity of TPDs towards Cu (II) and Zn (II) ions, the acid–base behavior of all compounds has been also evaluated.

The study of complexation was conducted by UV–Vis and fluorescence spectroscopy as well as using potentiometric method. The data were collected by titration where the pH measurement was conducted with glass electrode in 0.1 M NaClO₄ as ionic medium. Processing the potentiometric data,^[39] in absence of metals, the relative protolytic constants were obtained (Table 2) as well as from the acid constants were built up the distribution curves for all the species present in these systems (Fig. 3).

The elaboration of the data collected in presence of metals agrees with the results summarized in Table 3. Interestingly, all derivatives (**19** – **21** and **25** – **27**) showed a strong chelating ability for both metal ions, with stability constants in the range of 10^{6.5} – 10^{20.2}.

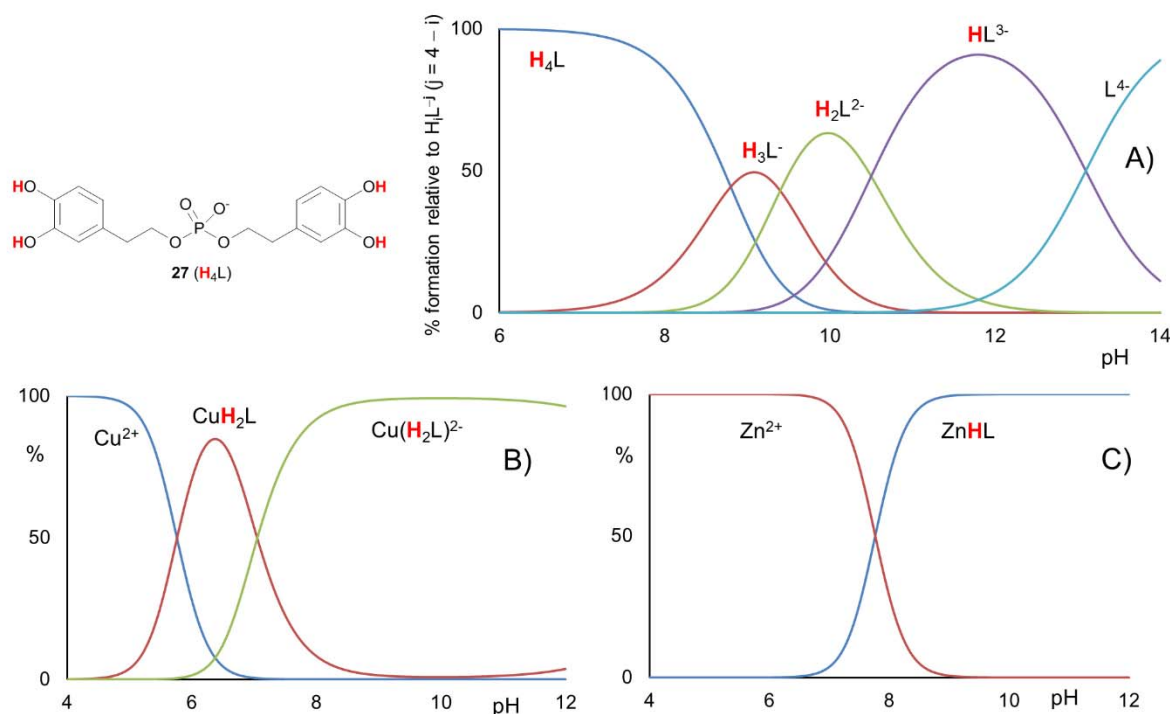


Figure 3. A) Distribution diagram of proteolytic species for compound **27** (H₄L) in 0.1 M NaClO₄; B) Distribution diagram of solutions containing 1.0 × 10⁻⁴ M Cu(II) and 2.0 × 10⁻⁴ M of compound **27** in 0.1 M NaClO₄, and C) Zn(II) and 2.0 × 10⁻⁴ M of compound **27** in 0.1 M NaClO₄.

Table 2 Acidity constants for Tyrosol–based Phosphodiester Derivatives (TPDs)

Compound	19	20	21	25	26	27
pK_{a1}	9.8 ± 0.1	9.2 ± 0.1	9.0 ± 0.1	8.5 ± 0.1	9.5 ± 0.1	8.8 ± 0.1
pK_{a2}	10.1 ± 0.2	10.6 ± 0.2	10.0 ± 0.2	10.5 ± 0.2	11.3 ± 0.2	9.4 ± 0.2
pK_{a3}	–	–	–	13.1 ± 0.5	13.0 ± 0.5	10.5 ± 0.3
pK_{a4}	–	–	–	–	–	13.1 ± 0.5

FULL PAPER

Table 3 Logarithm of stability constants relative to equilibria:
 $p \text{ Me}^{2+} + q \text{ H}_n\text{L} = \text{Me}_p\text{H}^r (\text{H}_n\text{L})_q + r \text{ H}^+$

Me ²⁺	Species (p, q, r)	25	26	27
Cu (II)	(1, 1, 2)	-8.0±0.5	-9.3±0.8	-8.7±0.2
	(1, 2, 4)	-17.8±0.8	-	-19.5±0.8
Zn (II)	(1, 1, 2)	-12.5±0.1	-12.7±0.2	-12.8±0.4

According to the results reported in Tables 2 and 3, the stability constants of all the complexes for Cu (II) and Zn (II) with TPDs are reported in Table 4.

From the distribution diagram of the Cu (II) – **27** system, shown in Fig. 3 (B), a prevalence of free metal is observed at pH until 5, while there is a prevalence of the CuH₂L complex at pH range 5 - 7 (which reaches a maximum of about 80%). UV spectra shown a similar profile for all the compounds. In particular, UV spectra of compound **27** in absence of complexation (Fig. 4), presents two typical phenolic group absorptions, at 220 nm ($\epsilon = 485\text{cm}^{-1}\text{M}^{-1}$) and 280 nm ($\epsilon = 860\text{cm}^{-1}\text{M}^{-1}$), which show minimal variations with the increase of pH.^[40] On the other hand, at pH greater than 7, the Cu (H₂L)₂²⁻ species is the only one present (greater than 95%). For the Zn (II) – **27** system, Fig. 3 (C), the free metal represents the prevalent specie until pH 7, while the ZnHL complex species becomes considerable at pH greater than 8.

Table 4 Summary of TPDs stability constants

Me ²⁺	TPD	Equilibrium	log (K _{eq})
Cu ²⁺	25	$\text{Cu}^{2+} + \text{HL}^{2-} \rightleftharpoons \text{CuHL}$	11.0
		$\text{Cu}^{2+} + 2 \text{HL}^{2-} \rightleftharpoons \text{Cu}(\text{HL})_2^{2-}$	20.2
	26	$\text{Cu}^{2+} + \text{HL}^{2-} \rightleftharpoons \text{CuHL}$	11.5
		27	$\text{Cu}^{2+} + \text{H}_2\text{L}^{2-} \rightleftharpoons \text{CuH}_2\text{L}$
$\text{Cu}^{2+} + 2 \text{H}_2\text{L}^{2-} \rightleftharpoons \text{Cu}(\text{H}_2\text{L})_2^{2-}$	16.9		
Zn ²⁺	25	$\text{Zn}^{2+} + \text{HL}^{2-} \rightleftharpoons \text{ZnHL}$	6.5
		26	$\text{Zn}^{2+} + \text{H}_2\text{L}^{2-} \rightleftharpoons \text{ZnH}_2\text{L}$
	27		$\text{Zn}^{2+} + \text{HL}^{2-} \rightleftharpoons \text{ZnHL}$

In presence of metal ions, a slight increase of absorbance upon complexation together with a bathochromic shift of the absorption band at 280 nm experiences. This effect is more evident with Cu²⁺ ions, probably thanks to the greater stability of the complex. Similar behavior is also present in the other compounds. This effect is more evident with Cu²⁺ ions, probably thanks to the greater stability of the complex.

Spectrofluorimetric measurements, performed on the same solutions showed a much more marked decrease in intensity (Fig. 4) in the presence of metal cations with respect to free compound **27** (depending on the pH). Also, in these measurements a greater variation was observed in the presence of Cu²⁺ ions.

Discussion

An investigation of the potentialities as neuroprotective agents of new Tyrosol-based phosphodiester derivatives (TPDs) has been carried out in order to identify new molecules to contrast Alzheimer's disease (AD) neurotoxicity by acting at different levels of the neurotoxic cascade. Strong relationships exist between A β and bio-metals, in fact experimental evidence indicates that metals might play a major role in the aggregation/precipitation of A β soluble oligomers.^{[41],[42]} Metal-ion-chelation was suggested to prevent Zn (II) and Cu (II) ions-induced A β aggregation and oxidative stress, both implicated in the pathophysiology of AD.

In the light of these considerations, antioxidant activity, A β anti-aggregation behaviour and bio-metal chelating capacity of TPDs were evaluated. In all cases the TPDs showed a greater or similar radical scavenger activity to that of the monomer units contained in them (Table 1).

Recently, combining ThT assays and MD simulations to study A β aggregation in the presence of tyrosol (TYR), 3-hydroxytyrosol (HDT) and 3-methoxytyrosol (homovanillyl alcohol - HVA), we have shown that while TYR and HVA catalyze fibril formation, HDT is a potent inhibitor of A β amyloid growth.^[26] According to these data, TPDs which contain two TYR or HVA moieties or a combination of both of them (TYR-*p*-TYR **19**, TYR-*p*-HVA **20** and HVA-*p*-HVA **21**), catalyzed the aggregation phenomenon as the parental monomers. These compounds reduced the lag phase and increased the total amount of the formed fibers at all tested peptide/ligand ratios (Fig. S1). Interestingly, TPDs that contain the monomer HDT (HDT-*p*-TYR **25**, HDT-*p*-HVA **26** and HDT-*p*-HDT **27**), presented a bimodal behavior, producing an acceleration or an inhibition of the aggregation depending on the concentration of dimer ligand. The efficacy of inhibiting the aggregation is only present at the higher tested peptide ligand molar ratios (1:1 and in some cases 1:0.5) while the ability to favor the aggregation of HVA and TYR counterbalances the catechol properties at the smaller tested ratio (1:0.25). Analyzing all data, it appears clear that the catechol moiety is responsible for the inhibitory effect on A β aggregation of the compounds that contain it.

The role of the catecholic moiety is also evident from the excellent Cu (II) and Zn (II) chelating capacity of the derivatives that contain HDT (**25** - **27**). Potentiometric measurements showed the formation of complexes with very high stability constants in the range of 10^{6.5} – 10^{20.2}. This behavior is also reflected in the spectrofluorimetric analysis, in which the presence of the metal, generates a very marked decrease in intensity as evidence of the participation of aromatic moieties in the formation of complex. This effect is more evident with Cu²⁺ ions, probably thanks to the greater stability of the complex.

For both metals the formation of complexes with stoichiometry 1: 1 were observed. While, for compounds **25** and **27**, Cu (II) complexes with stoichiometry 2: 1 were also observed. This last result could be due to the participation of two catecholic moieties to chelation with Cu (II) ion.

Conclusion

In conclusion, we have synthesized new tyrosol derivatives (TPDs) starting from three well known and abundant phenylethanoid alcohols: tyrosol (TYR), homovanillyl (HVA) and

FULL PAPER

hydroxytyrosol (HDT) alcohols. Starting from suitable protected tyrosol building blocks and exploiting the well-established phosphoramidite chemistry, we have developed an efficient synthetic strategy to obtain new tyrosol derivatives of natural metabolites known for their potential use in prevention of AD. The antioxidant activity (ABTS^{•+} test) of TPDs resulted generally greater than that of the precursors. Initially, TPDs were tested by thioflavin-T fluorescence assay to evaluate their A β ₄₀ aggregation inhibitory activity. Interestingly, TPDs that contain the HDT moieties (**25** – **27**), presented a bimodal behavior, producing an acceleration or an inhibition of the aggregation depending on the concentration of dimer ligands. Instead, dimers containing TYR or

HVA moieties (**19** – **21**), catalyzed the aggregation phenomenon as the monomeric precursors. These results show, in agreement with our previous studies, that the catechol group is crucial for the inhibition of A β aggregation; consequently, dimers that contain this moiety resulted strong inhibitors of A β aggregation. Based on these interesting antiaggregant activities, the ability of dimers **25** – **27** to complex Cu(II) and Zn(II) ions has been also investigated by potentiometric and UV spectrophotometric analyses. Although with different behaviour, all TPDs showed a strong chelating ability for both metal ions forming complexes with high stability constants in the range of 10^{6.5} – 10^{20.2}.

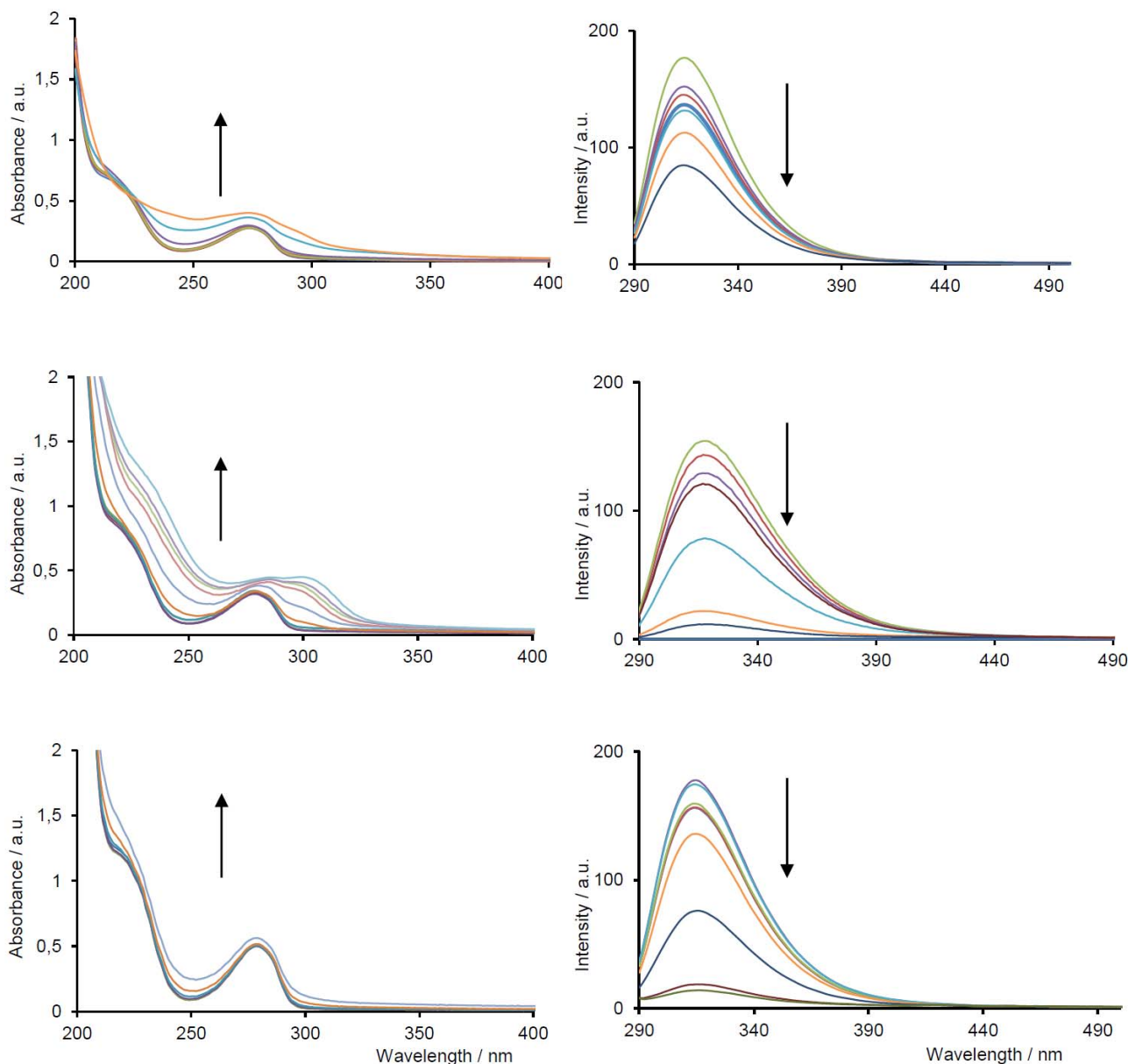


Fig. 4 UV spectra (on the left) and fluorescence spectra (on the right) of solution with composition: A, D) 0.90 mM of compound **27** (pH: from 6.59 to 10.84); B, E) 0.90-mM of compound **27** and 0.45-mM Cu(II) (pH: from 2.68 to 8.29); C, F) 0.90-mM of compound **27** and 0.45-mM Zn(II) (pH: from 3.36 to 7.57).

FULL PAPER

The good chelating ability, as well as, the possibility to modulate the anti-fibrillogenic activity of new derivative (dimers or conjugates), using building blocks with catecholic functions, opens up perspectives to the synthesis of new phosphodiester conjugates with hydroxytyrosol or caffeoyl alcohol, as promising AD agents.

Experimental Section

General methods

All chemicals were purchased from Sigma–Aldrich (Italy) except for hydroxytyrosol that was synthesized according to reported in the literature. HPLC–grade CH₃CN and CH₃OH were purchased from Carlo Erba Reagents and Sigma–Aldrich, respectively. The Aβ_{1–40} peptide was purchased from Genscript.

Reactions were monitored by TLC (precoated silica gel plates F254, Merck) and column chromatography (Merck Kieselgel 60, 70–230 mesh). HPLC analysis was performed with a Shimadzu LC–8A PLC system equipped with a Shimadzu SCL–10A VP System control and a Shimadzu SPD–10A VP UV–Vis detector. HPLC analysis were carried out on Phenomenex Luna RP18 column (5 μm particle size, 4.6 mm × 150 mm i.d.) using a gradient that started at 5% of CH₃CN in 0.1 M Ammonium Acetate in H₂O (pH 7.0) for 5 min and increased to 100% of ACN over 30 min at a flow rate of 0.8 mL/min with detection at 260 nm. For ESI–MS analysis, a Waters Micromass ZQ Instrument equipped with an electrospray source was used.

For Aβ aggregation experiments, samples were prepared by adding 1–2 μL of the studied molecules stock solutions in water or DMSO to 50 μL of ThT 20 μM in PBS (phosphate 10 mM, pH 7.4, 100 mM NaCl). Experiments were carried out in 384–well plates. Immediately after addition of Aβ_{1–40} (20 μM, final concentration) time traces were recorded using a Varioskan plate reader (ThermoFisher, Waltham, MA) with λ_{exc} 440 nm and λ_{em} 480 nm at 37 °C. Each experiment was performed in triplicate.

The potentiometric titrations were conducted in an air–bath thermostat kept at (25.00 ± 0.05) °C. A programmable computer–controlled data acquisition unit 3421A, supplied by Hewlett and Packard, was used to perform the potentiometric measurements. The glass electrodes were Metrohm (Herisau, Switzerland) of 60102–100 type and Ag/AgCl electrode was utilized as reference. The EMF values were measured with a precision of ± 0.01 mV using a Keithley 642 type Digital Electrometer.

UV–Vis spectra were recorded by model Cary 5000 Spectrophotometer by Varian C., from 200 to 600 nm (optical path 0.2 cm) at 25.0 °C, under a constant flow of nitrogen.

Fluorescence spectra were obtained using a JASCO spectrofluorimeter model FP–750, from 200 to 600 nm (optical path 0.2 cm).

Syntheses of full protected intermediates 4 – 6: general procedure.

To a solution of the compound 1 (2 or 3; 7.2 mmol) in DMF (15 mL), 4.0 mL triethylamine (32.0 mmol; 2.2 equiv. for each OH group) and 3.57 g of TBDMSCl (23.7 mmol; 1.1 equiv. for each OH group) were added and stirred at r.t. for 3 h. The reaction was quenched adding MeOH and extracted with H₂O/AcOEt. The combined organic phases were washed with sat. NaHCO₃ and brine, dried over anhydrous MgSO₄, and evaporated under

reduced pressure. The residue was purified by flash column chromatography on silica gel (Hexane/AcOEt 80:20 v/v) to give the compound 4 (5 or 6) in quantitative yield as a colourless oil.

Compound 4 ¹H NMR (400 MHz, CDCl₃): δ 7.08 (2H, d, *J* 8.5 Hz, H–2 and H–6), 6.78 (2H, d, *J* 8.5 Hz, H–3 and H–5), 3.80 (2H, t, *J* 6.8 Hz, H–8), 2.78 (2H, t, *J* 6.8 Hz, H–7), 1.01 (9H, s, (CH₃)₃CSiOAr), 0.90 (9H, s, (CH₃)₃CSiOCH₂), 0.21 (6H, s, (CH₃)₂SiOAr), 0.005 (6H, s, (CH₃)₂SiOCH₂). ¹³C NMR (100 MHz, CDCl₃): δ 153.9, 131.9, 130.0, 119.8, 64.8, 38.8, 25.9, 25.7, 18.4, 18.2, –4.4, –5.4. MS (ESI⁺): calcd. for C₂₀H₃₉O₂Si₂ [M+H]⁺ 367.25, found 367.48.

Compound 5 ¹H NMR (400 MHz, CDCl₃): δ 6.77 (1H, d, *J* 8.4 Hz, H–5), 6.73 (1H, d, *J* 2.2 Hz, H–2), 6.65 (1H, dd, *J* 8.4, 2.2 Hz, H–6), 3.81 (3H, s, OCH₃), 3.80 (2H, t, *J* 6.7 Hz, H–8), 2.76 (2H, t, *J* 6.9 Hz, H–7), 1.01 (9H, s, (CH₃)₃CSiOAr), 0.89 (9H, s, (CH₃)₃CSiOCH₂), 0.16 (6H, s, (CH₃)₂SiOAr), 0.005 (6H, s, (CH₃)₂SiOCH₂). ¹³C NMR (100 MHz, CDCl₃): δ 150.9, 143.6, 131.8, 121.1, 120.9, 113.0, 63.7, 55.5, 38.9, 25.7, 18.4, 18.2, –4.6, –5.5. MS (ESI⁺): calcd. for C₂₁H₄₁O₃Si₂ [M+H]⁺ 397.26, found 397.55.

Compound 6 ¹H NMR (400 MHz, CDCl₃): δ 6.75 (1H, d, *J* 8.3 Hz, H–5), 6.70 (1H, d, *J* 2.1 Hz, H–2), 6.65 (1H, dd, *J* 8.3, 2.2 Hz, H–6), 3.78 (2H, t, *J* 7.1 Hz, H–8), 2.72 (2H, t, *J* 7.1 Hz, H–7), 1.01 (9H, s, (CH₃)₃CSiOAr), 1.00 (9H, s, (CH₃)₃CSiOAr), 0.90 (9H, s, (CH₃)₃CSiOCH₂), 0.21 (6H, s, (CH₃)₂SiOAr), 0.20 (6H, s, (CH₃)₂SiOAr), 0.02 (6H, s, (CH₃)₂SiOCH₂). ¹³C NMR (100 MHz, CDCl₃): δ 146.4, 145.1, 132.3, 122.1, 122.0, 120.8, 64.8, 39.0, 26.0, 18.4, 18.4, 18.3, –4.0, –4.1, –5.3. MS (ESI⁺): calcd. for C₂₆H₅₃O₃Si₃ [M+H]⁺ 497.33, found 497.39.

Synthesis of intermediates 7 – 9. General procedure of the deprotection

2.20 mmol TBDMS ether 4 (5 or 6) were added to a round bottomed flask and diluted to 0.1 M concentration in MeOH. Once the substrate dissolved, 1 wt% (10 mg/mL) of I₂ was added. Reaction progress was monitored by TLC (DCM/MeOH 90:10 v/v). Upon consumption of the alcoholic silyl ether, solid Na₂S₂O₃ was added and the heterogeneous mixture stirred until the I₂ color had dissipated. The methanolic solution was then diluted with DCM and washed with saturated aqueous NaHCO₃. Drying over anhydrous MgSO₄, filtering, and evaporation to dryness give material that was then purified by flash column chromatography on silica gel (DCM/MeOH 90:10 v/v) to give compound 7 (8 or 9) in good yield.

Compound 7 (478.1 mg, 1.89 mmol, 86% yield) ¹H NMR (400 MHz, CDCl₃): δ 7.10 (2H, d, *J* 8.6 Hz, H–2 and H–6), 6.81 (2H, d, *J* 8.5 Hz, H–3 and H–5), 3.84 (2H, t, *J* 6.7 Hz, H–8), 2.82 (2H, t, *J* 6.6 Hz, H–7), 1.00 (9H, s, (CH₃)₃CSiOAr), 0.21 (6H, s, (CH₃)₂SiOAr). ¹³C NMR (100 MHz, CDCl₃): δ 154.3, 130.9, 130.0, 120.2, 63.8, 38.4, 25.7, 18.2 –4.4. MS (ESI⁺): calcd. for C₁₄H₂₅O₂Si [M+H]⁺ 253.16, found 253.86.

Compound 8 (515.3 mg, 82% yield) ¹H NMR (400 MHz, CDCl₃): δ 6.81 (1H, d, *J* 8.0 Hz, H–5), 6.74 (1H, d, *J* 1.9 Hz, H–2), 6.69 (1H, dd, *J* 8.0, 2.1 Hz, H–6), 3.84 (2H, t, *J* 6.5 Hz, H–8), 3.82 (3H, s, OCH₃), 2.81 (2H, t, *J* 6.6 Hz, H–7), 1.02 (9H, s, (CH₃)₃CSiOAr), 0.17 (6H, s, (CH₃)₂SiOAr). ¹³C NMR (100 MHz, CDCl₃): δ 150.9, 143.7, 131.8, 121.1, 120.9, 113.0, 63.7, 55.5, 38.9, 25.7, 18.4, –4.6. MS (ESI⁺): calcd. for C₁₅H₂₇O₃Si [M+H]⁺ 283.17, found 283.11.

Compound 9 (699.0 mg, 83% yield) ¹H NMR (400 MHz, CDCl₃): δ 6.79 (1H, d, *J* 8.1 Hz, H–5), 6.73 (1H, d, *J* 2.1 Hz, H–2), 6.68

FULL PAPER

(1H, dd, *J* 8.0, 2.1 Hz, H-6), 3.80 (2H, t, *J* 6.8 Hz, H-8), 2.76 (2H, t, *J* 6.7 Hz, H-7), 1.02 and 1.01 (18H, s, (CH₃)₃CSiOAr), 0.23 and 0.22 (12H, s, (CH₃)₂SiOAr). ¹³C NMR (100 MHz, CDCl₃): δ 146.8, 145.5, 131.3, 121.9, 121.8, 121.0, 63.8, 38.5, 25.9, 18.4, -4.0, -4.1. MS (ESI⁺): calcd. for C₂₀H₃₉O₃Si₂ [M+H]⁺ 383.24, found 383.55.

Syntheses of phosphoramidites 10 – 12: general procedure

To TBDMS ether **7** (**8** or **9**; 0.93 mmol) dissolved in anhydrous DCM (7 mL), DIEA (516 μL, 3.70 mmol) and then 2-cyanoethyl-N,N-diisopropylamino-chlorophosphoramidite (250 μL, 0.39 mmol) were added. Reaction progress was monitored by TLC (Hexane/AcOEt 80:20 v/v). After 1 h, the solution was diluted with AcOEt, and the organic phase was washed twice with brine and then concentrated. Column chromatography of the residue (Hexane/AcOEt 80:20, v/v with 1% TEA) afforded desired compound **10** (**11** or **12**; 0.24 mmol) in good yields.

Compound **10** (309.0 mg, 0.66 mmol, 72% yield) ¹H NMR (400 MHz, CDCl₃): δ 7.09 (2H, d, *J* 8.5 Hz, H-2 and H-6), 6.78 (2H, d, *J* 8.5 Hz, H-3 and H-5), 3.91–3.76 (4H, m, CNCH₂CH₂OP and H-8), 3.65–3.56 (2H, m, [(CH₃)₂CH]₂N), 2.87 (2H, t, *J* 7.0 Hz, H-7), 2.60 (2H, t, *J* 6.6 Hz, CNCH₂CH₂OP), 1.20 (6H, d, *J* 6.7 Hz, [(CH₃)₂CH]₂N), 1.17 (6H, d, *J* 6.7 Hz, [(CH₃)₂CH]₂N), 1.00 (9H, s, (CH₃)₃CSiOAr), 0.20 (6H, s, (CH₃)₂SiOAr). ¹³C NMR (100 MHz, CDCl₃): δ 154.1, 131.3, 129.9, 119.9, 117.6, 64.6, 64.5, 58.4, 58.2, 43.1, 43.0, 37.1, 37.0, 25.7, 24.8, 24.7, 24.6, 24.5, 20.4, 20.3, 18.2, -4.4. ³¹P NMR (161.98 MHz, CDCl₃): δ 147.3. MS (ESI⁺): calcd. for C₂₃H₄₂N₂O₃PSi [M+H]⁺ 453.27, found 453.39.

Compound **11** (481.7 mg, 0.63, 68% yield) ¹H NMR (400 MHz, CDCl₃): δ 6.78 (1H, d, *J* 8.1 Hz, H-5), 6.74 (1H, d, *J* 1.8 Hz, H-2), 6.68 (1H, dd, *J* 8.0, 1.9 Hz, H-6), 3.92–3.72 (4H, m, CNCH₂CH₂OP and H-8), 3.81 (3H, s, OCH₃), 3.65–3.56 (2H, m, [(CH₃)₂CH]₂N), 2.87 (2H, t, *J* 7.0 Hz, H-7), 2.60 (2H, t, *J* 6.6 Hz, CNCH₂CH₂OP), 1.19 (6H, d, *J* 6.7 Hz, [(CH₃)₂CH]₂N), 1.16 (6H, d, *J* 6.7 Hz, [(CH₃)₂CH]₂N), 1.01 (9H, s, (CH₃)₃CSiOAr), 0.16 (6H, s, (CH₃)₂SiOAr). ¹³C NMR (100 MHz, CDCl₃): δ 150.7, 143.4, 132.0, 121.2, 120.7, 117.7, 113.1, 64.7, 64.5, 58.4, 58.2, 55.5, 43.1, 43.0, 37.5, 37.4, 25.7, 24.7, 24.6, 24.5, 20.4, 20.3, 18.4, -4.6. ³¹P NMR (161.98 MHz, CDCl₃): δ 147.3. MS (ESI⁺): calcd. for MS (ESI⁺): calcd. for C₂₄H₄₄N₂O₄PSi [M+H]⁺ 483.28, found 483.37.

Compound **12** (487.0 mg, 0.84, 90% yield) ¹H NMR (400 MHz, CDCl₃): δ 6.76 (1H, d, *J* 8.1 Hz, H-5), 6.70 (1H, d, *J* 1.9 Hz, H-2), 6.67 (1H, dd, *J* 8.0, 2.1 Hz, H-6), 3.88–3.70 (4H, m, CNCH₂CH₂OP and H-8), 3.66–3.56 (2H, m, [(CH₃)₂CH]₂N), 2.82 (2H, t, *J* 7.3 Hz, H-7), 2.62 and 2.61 (2H, t, *J* 6.6 and 6.4 Hz, CNCH₂CH₂OP), 1.20 (6H, d, *J* 6.8 Hz, [(CH₃)₂CH]₂N), 1.17 (6H, d, *J* 6.8 Hz, [(CH₃)₂CH]₂N), 1.01 (9H, s, (CH₃)₃CSiOAr), 1.00 (9H, s, (CH₃)₃CSiOAr), 0.21 (6H, s, (CH₃)₂SiOAr), 0.20 (6H, s, (CH₃)₂SiOAr). ¹³C NMR (100 MHz, CDCl₃): δ 146.5, 145.3, 131.5, 121.9, 121.8, 120.8, 117.6, 64.6, 64.4, 58.5, 58.3, 43.1, 43.0, 37.2, 37.1, 26.0, 24.7, 24.6, 24.5, 24.4, 20.4, 20.3, 18.5, 18.4, -4.1. ³¹P NMR (161.98 MHz, CDCl₃): δ 147.2. MS (ESI⁺): calcd. for C₂₉H₅₆N₂O₄PSi₂ [M+H]⁺ 583.35, found 583.43.

Syntheses of Phosphotriester-linked Tyrosol dimers (13 – 15): general coupling procedure

The coupling reactions between the phosphoramidites (**10** – **12**) and the appropriately protected tyrosol building blocks (**7** – **9**) were carried out by suspending derivative **7** (**8** or **9**, 0.76 mmol) in a 0.25 M solution of DCI in ACN (4.5 mL 1.12 mmol) with 3–Å

molecular sieves. After a few min, each mixture was added to suitable phosphoramidite **10** (**11** or **12**, 0.70 mmol) dissolved in 1 mL of DCM and the solution was stirred for 3 h. Once the reaction appeared to be complete by TLC (Hexane/AcOEt 80:20, v/v), 150 μL (0.82 mmol) of a TBHP solution in decane (5.5 M) was added to the mixture, and after 1 h, the solvent was removed under vacuum. The crude material was then purified by column chromatography (Hexane/AcOEt 70:30 to 50:50 v/v) afforded desired compound **13** (**14** or **15**) in good yields.

Compound **13** (338.0 mg, 0.55 mmol, 78% yield) ¹H NMR (400 MHz, CDCl₃): δ 7.07 (4H, d, *J* 8.6 Hz, H-2', H-6 and H-6'), 6.78 (4H, d, *J* 8.5 Hz, H-3, H-3', H-5 and H-5'), 4.17 (4H, q, *J* 7.0 Hz, H-8 and H-8'), 4.01 (1H, t, *J* 6.2 Hz, CNCH₂CH₂OP), 3.99 (1H, t, *J* 6.2 Hz, CNCH₂CH₂OP), 2.89 (4H, t, *J* 7.5 Hz, H-7 and H-7') 2.58 (2H, t, *J* 6.2 Hz, CNCH₂CH₂OP), 0.99 (18H, s, (CH₃)₃CSiOAr), 0.19 (12H, s, (CH₃)₂SiOAr). ¹³C NMR (100 MHz, CDCl₃): δ 154.5, 130.0, 129.5, 120.1, 116.5, 68.7, 68.6, 61.6, 61.5, 35.8, 35.7, 25.7, 19.6, 19.5, 18.2, -4.4. ³¹P NMR (161.98 MHz, CDCl₃): δ -2.1. MS (ESI⁺): calcd. for C₃₁H₅₁NO₆PSi₂ [M+H]⁺ 620.30, found 620.88.

Compound **14** (372.5 mg, 0.57 mmol, 82% yield) ¹H NMR (400 MHz, CDCl₃): δ 7.05 (2H, d, *J* 8.6 Hz, H-2' and H-6'), 6.77 (3H, d, *J* 8.6 Hz, H-5, H-3' and H-5'), 6.71 (1H, d, *J* 2.0 Hz, H-2), 6.65 (1H, dd, 8.0, 2.0 Hz, H-6), 4.18 (4H, m, H-8 and H-8'), 3.99 (2H, q, *J* 6.3 Hz, CNCH₂CH₂OP), 3.77 (3H, s, OCH₃), 2.88 (4H, t, *J* 6.4 Hz, H-7 and H-7'), 2.58 (2H, t, *J* 6.3 Hz, CNCH₂CH₂OP), 1.00 (9H, s, (CH₃)₃CSiOAr), 0.98 (9H, s, (CH₃)₃CSiOAr), 0.17 (6H, s, (CH₃)₂SiOAr), 0.13 (6H, s, (CH₃)₂SiOAr). ¹³C NMR (100 MHz, CDCl₃): δ 154.5, 150.8, 143.8, 130.3, 130.0, 129.9, 129.5, 121.2, 120.8, 120.1, 116.5, 113.0, 68.7, 68.5, 61.6, 61.5, 55.5, 36.3, 36.2, 35.8, 25.7, 25.6, 19.5, 18.5, -4.4, -4.6. ³¹P NMR (161.98 MHz, CDCl₃): δ -2.0. MS (ESI⁺): calcd. for C₃₃H₅₅NO₈PSi₂ [M+H]⁺ 680.32, found 680.55.

Compound **15** (361.2 mg, 0.53 mmol, 76% yield) ¹H NMR (400 MHz, CDCl₃): δ 6.76 (2H, d, *J* 8.0 Hz, H-5 and H-5'), 6.70 (2H, d, *J* 1.9 Hz, H-2 and H-2'), 6.64 (2H, dd, *J* 8.0, 1.9 Hz, H-6 and H-6'), 4.19 (4H, q, *J* 7.1 Hz, H-8 and H-8'), 3.99 (1H, q, *J* 6.1 Hz, CNCH₂CH₂OP), 3.97 (1H, q, *J* 6.1 Hz, CNCH₂CH₂OP), 2.90 (4H, t, *J* 7.1 Hz, H-7 and H-7'), 2.58 (2H, t, *J* 6.0 Hz, CNCH₂CH₂OP), 0.98 (18H, s, (CH₃)₃CSiOAr), 0.13 (12H, s, (CH₃)₂SiOAr). ¹³C NMR (100 MHz, CDCl₃): δ 150.9, 143.8, 130.2, 121.2, 120.8, 116.5, 113.0, 68.6, 68.5, 61.6, 61.5, 55.5, 36.3, 36.2, 25.7, 18.4, -4.6. ³¹P NMR (161.98 MHz, CDCl₃): δ -2.0. MS (ESI⁺): calcd. for C₃₁H₅₁NO₆PSi₂ [M+H]⁺ 620.30, found 620.36.

Compound **16** (361.3 mg, 0.45 mmol, 65% yield) ¹H NMR (400 MHz, CDCl₃): δ 7.07 (2H, d, *J* 8.5 Hz, H-2' and H-6'), 6.79 (2H, d, *J* 8.4 Hz, H-3' and H-5'), 6.77 (1H, d, *J* 7.5 Hz, H-5), 6.70 (1H, d, *J* 2.1 Hz, H-2), 6.66 (1H, dd, 8.0, 2.2 Hz, H-6), 4.19 (4H, q, *J* 7.4 Hz, H-8 and H-8'), 4.05 (1H, t, *J* 6.3 Hz, CNCH₂CH₂OP), 4.03 (1H, t, *J* 6.3 Hz, CNCH₂CH₂OP), 2.91 (2H, t, *J* 7.0 Hz, H-7'), 2.86 (2H, t, *J* 7.1 Hz, H-7) 2.62 (2H, t, *J* 6.2 Hz, CNCH₂CH₂OP), 1.00, 0.99, 0.98 (27H, s, (CH₃)₃CSiOAr), 0.21, 0.20, 0.19 (18H, s, (CH₃)₃CSiOAr). ¹³C NMR (100 MHz, CDCl₃): δ 154.5, 146.7, 145.7, 130.0, 129.8, 129.4, 121.9, 121.8, 121.0, 120.1, 116.4, 68.8, 68.7, 61.6, 61.5, 36.9, 35.9, 25.9, 25.7, 19.6, 19.5, 18.4, 18.2, -4.1, -4.4. ³¹P NMR (161.98 MHz, CDCl₃): δ -2.0. MS (ESI⁺): calcd. for C₃₇H₆₅NO₇PSi₃ [M+H]⁺ 750.38, found 750.44.

Compound **17** (420.0 mg, 0.54 mmol, 77% yield) ¹H NMR (400 MHz, CDCl₃): δ 66.79, 6.77 (2H, d, *J* 8.0 Hz, H-5 and H-5'), 6.72, 6.69 (2H, d, *J* 2.1 Hz, H-2 and H-2'), 6.68, 6.66 (2H, dd, *J* 8.3, 2.2 Hz, H-6 and H-6'), 4.19 (4H, m, H-8 and H-8'), 4.05 (1H, t, *J*

FULL PAPER

6.3 Hz, CNCH₂CH₂OP), 4.03 (1H, t, *J* 6.3 Hz, CNCH₂CH₂OP), 3.80 (3H, s, OCH₃), 2.92 (2H, t, *J* 7.1 Hz, H-7), 2.90 (2H, t, *J* 7.1 Hz, H-7') 2.62 (2H, t, *J* 6.1 Hz, CNCH₂CH₂OP), 1.01, 1.00, 0.99 (27H, s, (CH₃)₃CSiOAr), 0.21, 0.20, 0.15 (18H, s, (CH₃)₃CSiOAr). ¹³C NMR (100 MHz, CDCl₃): δ 150.9, 146.7, 145.7, 143.9, 130.2, 129.8, 121.9, 121.8, 121.2, 121.0, 120.9, 116.4, 113.0, 68.7, 68.6, 61.6, 61.5, 55.5, 36.4, 36.3, 36.0, 35.9, 25.9, 25.7, 18.6, 18.4, -4.1, -4.6. ³¹P NMR (161.98 MHz, CDCl₃): δ -1.9. MS (ESI⁺): calcd. for C₃₈H₆₇NO₈PSi₃ [M+H]⁺ 780.39, found 780.46.

Compound **18** (443.2 mg, 0.50 mmol, 72% yield) ¹H NMR (400 MHz, CDCl₃): δ 6.77 (2H, d, *J* 8.0 Hz, H-5 and H-5'), 6.69 (2H, d, *J* 2.1 Hz, H-2 and H-2'), 6.66 (2H, dd, *J* 8.3, 2.2 Hz, H-6 and H-6'), 4.18 (4H, q, *J* 7.2 Hz, H-8 and H-8'), 4.07 (1H, t, *J* 6.1 Hz, CNCH₂CH₂OP), 4.05 (1H, t, *J* 6.1 Hz, CNCH₂CH₂OP), 2.86 (4H, t, *J* 7.1 Hz, H-7 and H-7'), 2.64 (2H, t, *J* 6.2 Hz, CNCH₂CH₂OP), 1.00, 0.99 (36H, s, (CH₃)₃CSiOAr), 0.20, 0.19 (24H, s, (CH₃)₂SiOAr). ¹³C NMR (100 MHz, CDCl₃): δ 146.7, 145.7, 129.8, 121.9, 121.8, 121.0, 116.3, 68.7, 68.6, 61.6, 61.5, 60.3, 36.0, 35.9, 25.9, 19.5, 18.4, -4.0. ³¹P NMR (161.98 MHz, CDCl₃): δ -1.9. MS (ESI⁺): calcd. for C₄₃H₇₉NO₈PSi₄ [M+H]⁺ 880.46, found 880.82.

Synthesis of Phosphate-linked Tyrosol dimers (19 – 21): deprotection procedure (method A)

To the dimer **13** (**14** or **15**; 0.34 mmol) dissolved in THF (2 mL) was added 1.0 mL of 1M NaOH water solution (1.0 mmol). After stirring for 4 h at r. t., the solution was adjusted to pH 3 with 1 M HCl and the solvent was removed under reduced pressure. The extracted was then purified by column chromatography (DCM/MeOH 50:50 v/v).

Compound **19** (91.8 mg, 0.25 mmol, 75% yield) ¹H NMR (400 MHz, CDCl₃): δ 7.03 (4H, d, *J* 8.4 Hz, H-2, H-2', H-6 and H-6'), 6.72 (4H, d, *J* 8.4 Hz, H-3, H-3', H-5 and H-5'), 3.90 (4H, q, *J* 6.9 Hz, H-8 and H-8'), 2.77 (4H, t, *J* 7.1 Hz, H-7 and H-7'). ¹³C NMR (100 MHz, CDCl₃): δ 155.4, 129.6, 129.2, 114.7, 66.2, 66.1, 36.1, 36.0. ³¹P NMR (161.98 MHz, CDCl₃): δ 0.56. MS (ESI⁺): calcd. for C₁₆H₂₀O₆P [M+H]⁺ 339.10, found 339.22 [M+H]⁺, 361.22 [M+Na]⁺, 377.59 [M+K]⁺.

Compound **20** (103.4 mg, 0.26 mmol, 78% yield) ¹H NMR (400 MHz, CDCl₃): δ 7.01 (2H, d, *J* 8.5 Hz, H-2' and H-6'), 6.82 (1H, d, *J* 1.8 Hz, H-2), 6.73 (1H, d, *J* 8.5 Hz, H-5), 6.71 (2H, d, *J* 8.5 Hz, H-3' and H-5'), 6.66 (1H, dd, *J* 8.1, 1.8 Hz, H-6), 3.93 (4H, m, H-8 and H-8'), 3.83 (3H, s, OCH₃), 2.76 (4H, q, *J* 7.1 Hz, H-7 and H-7'). ¹³C NMR (100 MHz, CDCl₃): δ 155.5, 147.3, 144.5, 130.1, 129.6, 129.1, 121.2, 114.8, 114.7, 112.4, 66.3, 66.2, 55.0, 36.4, 36.0. ³¹P NMR (161.98 MHz, CDCl₃): δ 0.30. MS (ESI⁺): calcd. for C₁₇H₂₂O₇P [M+H]⁺ 369.11, found 369.55 [M+H]⁺, 391.88 [M+Na]⁺, 407.65 [M+K]⁺.

Compound **21** (110.0 mg, 0.26 mmol, 77% yield) ¹H NMR (400 MHz, CDCl₃): δ 6.83 (2H, d, *J* 1.9 Hz, H-2 and H-2'), 6.72 (2H, d, *J* 8.0 Hz, H-5 and H-5'), 6.64 (2H, dd, *J* 8.0, 1.9 Hz, H-6 and H-6') 3.95 (4H, q, *J* 6.9 Hz, H-8 and H-8'), 3.80 (6H, s, OCH₃), 2.78 (4H, t, *J* 7.0 Hz, H-7 and H-7'). ¹³C NMR (100 MHz, CDCl₃): δ 147.3, 144.5, 130.0, 121.2, 114.7, 112.4, 66.3, 66.2, 55.0, 36.4, 36.3. ³¹P NMR (161.98 MHz, CDCl₃): δ 0.36. MS (ESI⁺): calcd. for C₁₈H₂₄O₈P [M+H]⁺ 399.12, found 399.23 [M+H]⁺, 421.68 [M+Na]⁺, 438.21 [M+K]⁺.

Synthesis of Phosphate-linked Tyrosol dimers (22 – 24): deprotection procedure (method B)

To a dimer **16** (**17** or **18**, 0.23 mmol) dissolved in THF (4 mL) was added 560 μL of a solution of Et₃N·3HF (3.45 mmol) The mixture

was stirred at room temperature for 3.5 h. Then, the reaction was worked up by removal of the solvent, redissolved on AcOEt. The solvent was removed under reduced pressure and the residue was purified by column chromatography on silica gel (DCM/MeOH 80:20 v/v, contained 0.05% TFA) to give a phosphotriester compounds **22** – **24**, in good yields. The obtained products were subsequently treated with a mix of ammonia/CH₃OH (1:1, v/v) at r.t for 30 min to removal the 2-cyanoethyl protecting group. The crude materials were then purified by column chromatography (DCM/MeOH 60:40 to 50:50 v/v).

Compound **22** (117.2 mg, 0.16 mmol, 68% yield) ¹H NMR (400 MHz, CDCl₃): δ 7.06 (2H, d, *J* 8.5 Hz, H-2' and H-6'), 6.75 (2H, d, *J* 8.5 Hz, H-3' and H-5'), 6.72 (1H, d, *J* 8.1 Hz, H-5), 6.70 (1H, d, *J* 2.1 Hz, H-2), 6.56 (1H, dd, 8.0, 2.2 Hz, H-6), 4.14 (4H, q, *J* 7.0 Hz, H-8 and H-8'), 3.96 (1H, q, *J* 6.3 Hz, CNCH₂CH₂OP), 3.94 (1H, q, *J* 6.3 Hz, CNCH₂CH₂OP), 2.85 (2H, t, *J* 6.7 Hz, H-7), 2.80 (2H, t, *J* 6.7 Hz, H-7'), 2.71 (2H, t, *J* 7.0 Hz, CNCH₂CH₂OP). ¹³C NMR (100 MHz, CDCl₃): δ 155.8, 144.9, 143.7, 129.8, 128.7, 127.9, 120.1, 115.8, 115.1, 115.0, 69.0, 68.9, 35.5, 35.3. ³¹P NMR (161.98 MHz, CDCl₃): δ -2.44. MS (ESI⁺): calcd. for C₁₉H₂₃NO₇P [M+H]⁺ 408.12, found 408.22 [M+H]⁺, 430.67 [M+Na]⁺, 446.19 [M+K]⁺.

Compound **23** (136.1 mg, 0.18 mmol, 79% yield) ¹H NMR (400 MHz, CDCl₃): δ 6.87 (1H, d, *J* 8.0 Hz, H-5), 6.85 (1H, d, *J* 8.0 Hz, H-5'), 6.79 and 6.71 (2H, d, H-2, H-2'), 6.66 and 6.52 (2H, dd, *J* 8.1, 2.0 Hz, H-6 and H-6'), 4.21 (4H, q, *J* 7.1 Hz, H-8 and H-8'), 3.98 (1H, t, *J* 6.4 Hz, CNCH₂CH₂OP), 3.96 (1H, t, *J* 6.2 Hz, CNCH₂CH₂OP), 3.83 (3H, s, OCH₃), 2.88 (2H, t, *J* 6.8 Hz, H-7), 2.78 (2H, t, *J* 7.1 Hz, H-7') 2.64 (2H, t, *J* 6.1 Hz, CNCH₂CH₂OP). ¹³C NMR (100 MHz, CDCl₃): δ 146.6, 144.4, 143.9, 143.2 129.0, 128.7, 121.7, 120.1, 115.8, 115.2, 114.9, 112.3, 69.0, 68.8, 62.3, 55.0, 36.2, 35.8. ³¹P NMR (161.98 MHz, CDCl₃): δ -2.6. MS (ESI⁺): calcd. for C₂₀H₂₅NO₈P [M+H]⁺ 438.13, found 438.40 [M+H]⁺, 460.68 [M+Na]⁺, 476.57 [M+K]⁺.

Compound **24** (88.0 mg, 0.10 mmol, 45% yield) ¹H NMR (400 MHz, CDCl₃): δ 6.73 (2H, d, *J* 8.1 Hz, H-5 and H-5'), 6.70 (2H, d, *J* 2.1 Hz, H-2 and H-2'), 6.55 (2H, dd, *J* 8.0, 2.0 Hz, H-6 and H-6'), 4.12 (4H, q, *J* 6.7 Hz, H-8 and H-8'), 3.95 (2H, q, *J* 5.9 Hz, CNCH₂CH₂OP), 2.78 (4H, t, *J* 6.7 Hz, H-7 and H-7'), 2.69 (2H, t, *J* 5.9 Hz, CNCH₂CH₂OP). ¹³C NMR (100 MHz, CDCl₃): δ 144.8, 143.6, 128.8, 120.2, 115.9, 115.2, 69.2, 69.0, 62.2, 62.1, 35.5, 35.4. ³¹P NMR (161.98 MHz, CDCl₃): δ -2.5. MS (ESI⁺): calcd. for C₁₉H₂₃NO₈P [M+H]⁺ 424.12, found 424.34 [M+H]⁺, 446.28 [M+Na]⁺, 462.81 [M+K]⁺.

Compound **25** (39.0 mg, 0.10 mmol, 65% yield) ¹H NMR (400 MHz, CDCl₃): δ 7.03 (2H, d, *J* 8.3 Hz, H-2' and H-6'), 6.71 (2H, d, *J* 8.3 Hz, H-3' and H-5'), 6.69 (2H, d, *J* 8.2 Hz, H-5), 6.67 (1H, m, H-2), 6.53 (1H, dd, 7.8, 1.8 Hz, H-6), 3.93 (4H, q, *J* 6.3 Hz, H-8 and H-8'), 2.78 (2H, t, *J* 6.8 Hz, H-7), 2.73 (2H, t, *J* 6.7 Hz, H-7'). ¹³C NMR (100 MHz, CDCl₃): δ 155.4, 144.7, 143.3, 129.9, 129.6, 129.1, 119.9, 115.8, 114.8, 114.7, 66.3, 66.2, 36.0, 35.9. ³¹P NMR (161.98 MHz, CDCl₃): δ -2.3. MS (ESI⁺): calcd. for C₁₆H₂₀O₇P [M+H]⁺ 355.09, found 355.38 [M+H]⁺, 377.12 [M+Na]⁺, 393.08 [M+K]⁺.

Compound **26** (41.6 mg, 0.10 mmol, 55% yield) ¹H NMR (400 MHz, CD₃OD): δ 6.79 (1H, d, *J* 1.9 Hz, H-2'), 6.72 (1H, d, *J* 7.8 Hz, H-5), 6.69 (1H, d, *J* 7.6 Hz, H-5'), 6.68 (1H, br s, H-2), 6.65 (1H, dd, *J* 7.8, 2.0 Hz H-6), 6.53 (1H, dd, *J* 7.6, 1.9 Hz H-6'), 3.94 (4H, m, H-8 and H-8'), 3.82 (3H, s, OCH₃), 2.80 (2H, t, *J* 6.8 Hz, H-7), 2.73 (2H, t, *J* 6.9 Hz, H-7'). ¹³C NMR (100 MHz, CD₃OD):

FULL PAPER

δ 147.4, 144.6, 144.5, 143.3, 130.0, 129.9, 121.1, 120.0, 115.8, 114.9, 114.7, 112.3, 66.4, 66.3, 55.0, 36.2, 36.0. ^{31}P NMR (161.98 MHz, CD_3OD): δ -3.0. MS (ESI⁺): calcd. for $\text{C}_{17}\text{H}_{22}\text{O}_8\text{P}$ $[\text{M}+\text{H}]^+$ 385.10, found 385.38 $[\text{M}+\text{H}]^+$, 407.36 $[\text{M}+\text{Na}]^+$, 423.57 $[\text{M}+\text{K}]^+$. Compound **27** (30.2 mg, 0.08 mmol, 71% yield) ^1H NMR (400 MHz, CD_3OD): δ 6.69 (2H, d, J 8.3 Hz, H-5 and H-5'), 6.68 (2H, d, J 2.2 Hz, H-2 and H-2'), 6.54 (2H, dd, J 7.9, 1.8 Hz, H-6 and H-6'), 3.96 (4H, q, J 6.6 Hz, H-8 and H-8'), 2.74 (4H, t, J 6.8 Hz, H-7 and H-7'). ^{13}C NMR (100 MHz, CD_3OD): δ 144.7, 143.4, 129.7, 120.0, 115.8, 114.9, 66.8, 66.7, 36.0, 35.9. ^{31}P NMR (161.98 MHz, CD_3OD): δ -2.1. MS (ESI⁺): calcd. for $\text{C}_{16}\text{H}_{20}\text{O}_8\text{P}$ $[\text{M}+\text{H}]^+$ 371.09, found 371.38 $[\text{M}+\text{H}]^+$, 393.46 $[\text{M}+\text{Na}]^+$, 409.38 $[\text{M}+\text{K}]^+$.

Radical scavenging test (ABTS^{•+})

The assays were carried out as already described by Bernini, R. et al.^[38] Firstly, an ABTS radical cation (ABTS^{•+}) stock solution was prepared. ABTS (30.7 mg) was dissolved in water (8.0 mL) to obtain a 7.0 mM solution. Then, 5.3 mg of $\text{K}_2\text{S}_2\text{O}_8$ were added and the mixture was kept in the dark at room temperature for 16 h to produce ABTS radical cation (ABTS^{•+}). After this time, the ABTS^{•+} solution was diluted with ethanol until to reach an absorbance value of 0.7 ± 0.02 at $\lambda = 734$ nm. Phenolic compounds to test were solubilized in ethanol to afford 0.04–0.4 mM solutions. For the radical scavenging assay, 950 μL of the ABTS^{•+} solution and 50 μL of ethanolic solutions of phenolic compounds were mixed at room temperature. After 10 min, the absorbance values at $\lambda = 734$ nm were registered. Three measurements were recorded for each concentration; each time blanks of pure solvent were run. Trolox was used as the antioxidant control; the results were expressed as Trolox Equivalent Antioxidant Capacity (TEAC), that is the concentration of antioxidant giving the same percentage inhibition of absorbance (%) of the radical cation at $\lambda = 734$ nm as 1.0 mM Trolox. A dose-response curve for was obtained plotting % of the ABTS^{•+} as function of range of concentrations of antioxidant compounds or Trolox. TEAC value is calculated dividing the gradient of the plot of the percentage inhibition of absorbance vs. concentration plot for the antioxidant in question by the gradient of the plot for Trolox. Results are expressed as means \pm standard deviations.

A β fibrillation kinetics: ThT assay

A β_{1-40} was monomerized by solubilizing it in HFIP (1 mg/mL), aliquoted (100 μL), frozen at -80 °C and lyophilized. To quantify A β , a lyophilized aliquot was solved in 20 μL of NaOH 1 mM and added to 180 μL of buffer (phosphate 10 mM, pH 7.4) and the absorbance was measured at 280 nm ($\epsilon_{280} = 1450 \text{ M}^{-1}\cdot\text{cm}^{-1}$). Samples for ThT assays were prepared by adding 1–2 μL of the corresponding TPD stock solutions (final ligand concentrations 5 μM , 10 μM or 20 μM) to 50 μL of ThT 20 μM in buffer (phosphate 10 mM, pH 7.4, NaCl 100 mM). Immediately after the addition of A β_{1-40} (20 μM , final concentration), time traces were recorded ($\lambda_{\text{exc}} = 440$ nm and $\lambda_{\text{em}} = 480$ nm) using a 384-well plate in a Varioskan plate reader (ThermoFisher, Waltham, MA) at 37 °C. A glass bead (diam. 1 cm) was added to each well, and the plate was shaken for 10 s before each read (600 shakes per minute with a diameter of the orbital movement of 1 mm). To exclude false ThT positive signals, controls in the absence of A β_{1-40} were also carried out for each tested condition. Each condition was tested in triplicate and kinetic curves were fitted with the following equation:

$$I = \frac{I_{\text{max}}}{1 + e^{(-k \cdot (t - t_{1/2}))}}$$

where I is the fluorescence intensity as function of time t , I_{max} corresponds with the maximum intensity of fluorescence, k is the apparent rate constant, $t_{1/2}$ and lag time (t_{lag}) represent the point in time where the signal reaches 50% and 10% of the amplitude of the transition, respectively. Data are expressed as the average of the kinetic parameters obtained by fitting each of the replicas and indicated as mean (standard error).

Acknowledgements

We acknowledge AIPRAS Onlus (Associazione Italiana per la Promozione delle Ricerche sull'Ambiente e la Salute umana) for grants in support of this investigation. S.G.V. is grateful to the European Union Horizon 2020 research and innovation program for funding her PhD fellowship under the Marie Skłodowska-Curie grant agreement INCIPIT n. 665403.

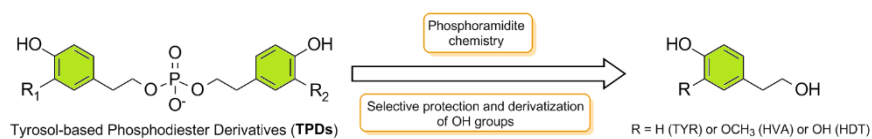
Keywords: Alzheimer's disease • amyloid beta • amyloid aggregation • hydroxytyrosol • dimer flavonoids.

- [1] D. J. Newman, G. M. Cragg, *J. Nat. Prod.* **2016**, *79*, 629–661.
- [2] K. Neha, M. R. Haider, A. Pathak, M. S. Yar, *Eur. J. Med. Chem.* **2019**, *178*, 687–704.
- [3] S. Quideau, D. Deffieux, C. Douat-Casassus, L. Pouységu, *Angew. Chemie Int. Ed.* **2011**, *50*, 586–621.
- [4] S. Losada-Barreiro, C. Bravo-Díaz, *Eur. J. Med. Chem.* **2017**, *133*, 379–402.
- [5] M. G. Savelieff, G. Nam, J. Kang, H. J. Lee, M. Lee, M. H. Lim, *Chem. Rev.* **2019**, *119*, 1221–1322.
- [6] K. Blennow, M. J. de Leon, H. Zetterberg, *Lancet* **2006**, *368*, 387–403.
- [7] F. Florenzano, C. Veronica, G. Ciasca, M. T. Ciotti, A. Pittaluga, G. Olivero, M. Feligioni, F. Iannuzzi, V. Latina, M. F. Maria Sciacca, A. Sinopoli, D. Milardi, G. Pappalardo, D. S. Marco, M. Papi, A. Atlante, A. Bobba, A. Borreca, P. Calissano, G. Amadoro, *Oncotarget* **2017**, *8*, 64745–64778.
- [8] F. Chiti, C. M. Dobson, *Annu. Rev. Biochem.* **2017**, *86*, 27–68.
- [9] J. A. Orellana, K. F. Shoji, V. Abudara, P. Ezan, E. Amigou, P. J. Sáez, J. X. Jiang, C. C. Naus, J. C. Sáez, C. Giaume, *J. Neurosci.* **2011**, *31*, 4962–4977.
- [10] G. Eskici, P. H. Axelsen, *Biochemistry* **2012**, *51*, 6289–6311.
- [11] M. G. Savelieff, S. Lee, Y. Liu, M. H. Lim, *ACS Chem. Biol.* **2013**, *8*, 856–865.
- [12] P. Faller, C. Hureau, G. La Penna, *Acc. Chem. Res.* **2014**, *47*, 2252–2259.
- [13] G. Grasso, A. M. Santoro, V. Lanza, D. Sbardella, G. R. Tundo, C. Ciaccio, S. Marini, M. Coletta, D. Milardi, *Coord. Chem. Rev.* **2017**, *347*, 1–22.
- [14] M. Stefani, S. Rigacci, *Int. J. Mol. Sci.* **2013**, *14*, 12411–12457.
- [15] B. Cheng, H. Gong, H. Xiao, R. B. Petersen, L. Zheng, K. Huang, *Biochim. Biophys. Acta - Gen. Subj.* **2013**, *1830*, 4860–4871.
- [16] A. Iraj, M. Khoshneviszadeh, O. Firuzi, M. Khoshneviszadeh, N. Edraki, *Bioorg. Chem.* **2020**, *97*, 103649.
- [17] Z. Dhouafii, K. Cuanalo-Contreras, E. A. Hayouni, C. E. Mays,

FULL PAPER

- C. Soto, I. Moreno-Gonzalez, *Cell. Mol. Life Sci.* **2018**, *75*, 3521–3538.
- [18] R. Taguchi, K. Hatayama, T. Takahashi, T. Hayashi, Y. Sato, D. Sato, K. Ohta, H. Nakano, C. Seki, Y. Endo, K. Tokuraku, K. Uwai, *Eur. J. Med. Chem.* **2017**, *138*, 1066–1075.
- [19] C. Lambruschini, D. Galante, L. Moni, F. Ferraro, G. Gancia, R. Riva, A. Traverso, L. Banfi, C. D'Arrigo, *Org. Biomol. Chem.* **2017**, *15*, 9331–9351.
- [20] M. Ramesh, P. Makam, C. Voshavar, H. Khare, K. Rajasekhar, S. Ramakumar, T. Govindaraju, *Org. Biomol. Chem.* **2018**, *16*, 7682–7692.
- [21] X. Zhang, X. He, Q. Chen, J. Lu, S. Rapposelli, R. Pi, *Bioorganic Med. Chem.* **2018**, *26*, 543–550.
- [22] M. M. Serafini, M. Catanzaro, M. Rosini, M. Racchi, C. Lanni, *Pharmacol. Res.* **2017**, *124*, 146–155.
- [23] R. Bernini, I. Carastro, F. Santoni, M. Clemente, *Antioxidants* **2019**, *8*, 174.
- [24] J. A. González-Correa, M. D. Navas, J. A. Lopez-Villodres, M. Trujillo, J. L. Espartero, J. P. De La Cruz, *Neurosci. Lett.* **2008**, DOI 10.1016/j.neulet.2008.09.022.
- [25] K. Taniguchi, F. Yamamoto, T. Arai, J. Yang, Y. Sakai, M. Itoh, N. Mamada, M. Sekiguchi, D. Yamada, A. Saitoh, F. Kametani, A. Tamaoka, Y. M. Araki, K. Wada, H. Mizusawa, W. Araki, *J. Alzheimer's Dis.* **2019**, *70*, 937–952.
- [26] V. Romanucci, S. García-Viñuales, C. Tempra, R. Bernini, A. Zarrelli, F. Lolicato, D. Milardi, G. Di Fabio, *Biophys. Chem.* **2020**, *265*, 106434.
- [27] R. Bernini, N. Merendino, A. Romani, F. Velotti, *Curr. Med. Chem.* **2013**, *20*, 655–670.
- [28] R. Bernini, M. S. Gilardini Montani, N. Merendino, A. Romani, F. Velotti, *J. Med. Chem.* **2015**, *58*, 9089–9107.
- [29] R. Bernini, I. Carastro, G. Palmi, A. Tanini, R. Zonefrati, P. Pinelli, M. L. Brandi, A. Romani, *J. Agric. Food Chem.* **2017**, *65*, 6506–6512.
- [30] F. Casamenti, M. Stefani, *Expert Rev. Neurother.* **2017**, *17*, 345–358.
- [31] F. Sarubbo, D. Moranta, G. Pani, *Neurosci. Biobehav. Rev.* **2018**, *90*, 456–470.
- [32] S. Molino, M. Dossena, D. Buonocore, F. Ferrari, L. Venturini, G. Ricevuti, M. Verri, *Life Sci.* **2016**, *161*, 69–77.
- [33] G. D'Andrea, M. Ceccarelli, R. Bernini, M. Clemente, L. Santi, C. Caruso, L. Micheli, F. Tirone, *FASEB J.* **2020**, *34*, 4512–4526.
- [34] E. Panel, A. Nda, *EFSA J.* **2011**, *9*, 2033.
- [35] R. Bernini, E. Mincione, M. Barontini, F. Crisante, *J. Agric. Food Chem.* **2008**, *56*, 8897–8904.
- [36] N. Pellegrini, F. Visioli, S. Buratti, F. Brighenti, *J. Agric. Food Chem.* **2001**, *49*, 2532–2538.
- [37] R. Bernini, F. Crisante, M. Barontini, D. Tofani, V. Balducci, A. Gambacorta, *J. Agric. Food Chem.* **2012**, *60*, 7408–7416.
- [38] R. Bernini, M. Barontini, V. Cis, I. Carastro, D. Tofani, R. Chiodo, P. Lupattelli, S. Incerpi, *Molecules* **2018**, *23*, 208.
- [39] P. GANS, A. SABATINI, A. VACCA, *Talanta* **1996**, *43*, 1739–1753.
- [40] G. De Tommaso, G. Malgieri, L. De Rosa, R. Fattorusso, G. D'Abrosca, A. Romanelli, M. Iuliano, L. D. D'Andrea, C. Isernia, *Dalt. Trans.* **2019**, *48*, 15184–15191.
- [41] M. Innocenti, E. Salvietti, M. Guidotti, A. Casini, S. Bellandi, M. L. Foresti, C. Gabbiani, A. Pozzi, P. Zatta, L. Messori, *J. Alzheimer's Dis.* **2010**, *19*, 1323–1329.
- [42] J. Mayes, C. Tinker-Mill, O. Kolosov, H. Zhang, B. J. Tabner, D. Allsop, *J. Biol. Chem.* **2014**, *289*, 12052–12062.

Table of Contents



New derivatives containing two tyrosol fragments linked through a phosphodiester bond. Interesting A β anti-aggregating activities and an excellent chelating ability of bio-metals as Cu (II) and Zn (II), whose regulation plays a key role in neurodegeneration processes, were found.